arXiv:nucl-th/0108043v1 17 Aug 2001

OITS 706
July 31, 2013

Centrality Dependence of Baryon and Meson Momentum Distributions in Proton-Nucleus Collisions

Rudolph C. Hwa[1] and C. B. Yang[1,2]
[1]*Institute of Theoretical Science and Department of Physics, University of Oregon, Eugene, OR 97403-5203, USA*
[2]*Institute of Particle Physics, Hua-Zhong Normal University, Wuhan 430079, P. R. China*

The proton and neutron inclusive distributions in the projectile fragmentation region of pA collisions are studied in the valon model. Momentum degradation and flavor changes due to the nuclear medium are described at the valon level using two parameters. Particle production is treated by means of the recombination subprocess. The centrality dependences of the net proton and neutron spectra of the NA49 data are satisfactorily reproduced. The effective degradation length is determined to be 17 fm. Pion inclusive distributions can be calculated without any adjustable parameters.

PACS Number(s): 25.75.Dw, 13.85.Ni

I. INTRODUCTION

The study of proton-nucleus (pA) collisions is important because they are tractable intermediaries between pp and AA collisions, when intense interest exists in discovering the extent to which the dense medium created in an AA collision differ from that of linear superpositions of pp collisions. One of the properties of pA collisions is that the momentum of the leading baryon in the projectile fragmentation region is degraded, a phenomenon commonly referred to, somewhat inappropriately, as baryon stopping. Such a transference of baryon number from the fragmentation to the central region contributes to the increase of matter density at mid-rapidity, thereby raising the likelihood of the formation of quark-gluon plasma. Thus it is important to understand the process of baryon momentum degradation and its dependence on nuclear size or centrality.

Since it is not feasible to perform first-principle parameter-free calculations of the momentum degradation at this point, experimental guidance is of crucial importance. Recently, several experiments have produced useful data on the subject, in particular, E910 and E941 at the AGS, and NA49 at the SPS [1]. It is the x_F dependences of the distributions of $p-\bar{p}$ and $n-\bar{n}$ that we shall focus on; moreover, their dependences on centrality will guide us in our determination of the nuclear effect on baryon momentum degradation.

The degradation of baryon momentum has been studied in various approaches before [2]-[8]. In Refs. [2]-[5] the investigations are done at the nucleon level, while in Refs. [6]-[8] the string model is the basis. Since it is questionable that the concept of color strings can be relevant in heavy-ion collisions where the abundance of color charges in the overlap region renders unlikely the development of constricted color flux tubes [9], our approach in this paper will be on the various levels of the constituents of the nucleon that are consistent with the parton model. More specifically, we shall use the valon model [10]-[12] to keep track of the momenta of the constituents and the recombination model [12, 13] to describe the hadronization of the partons. The valons play a role in the collision problem as the constituent quarks do in the bound-state problem. Thus a nucleon has three valons which carry all the momentum of the nucleon, while each valon has one valence quark and its own sea quarks and gluons. Although soft processes are non-perturbative, the valon model (including recombination) nevertheless provides a systematic way of calculating all subprocesses that contribute to a particular inclusive process. Some of the subprocesses can be identified with certain diagrams in other approaches, e.g., baryon junction and diquark breaking terms [7, 8].

The valon distributions in the proton will be determined by fitting the parton distributions at low Q^2. The effect of the nuclear medium on the valon distribution of the proton projectile will involve two parameters, one characterizing the momentum degradation and the other flavor flipping. The color indices are all averaged over, since multiple gluon interactions, as the projectile traverses the target nucleus, are numerous and uncomputable. Their effects are, however, quantified in terms of the number, ν, of target nucleons that participate in the pA collision. For that reason it is important that the experimental data must have centrality selection expressible in terms of the average $\bar{\nu}$.

The inclusive process $p+A\to p+X$ has been studied before in the valon model [14]. However, the pertinent data available at that time had no centrality cuts and were for fixed p_T [15]. Now, NA49 has p-Pb data on the production of $p, \bar{p}, n$ and $\bar{n}$ in the proton fragmentation region (with contribution from the nuclear target subtracted) for various values of $\bar{\nu}$ [1]. To extract more information from these refined data we have improved our formulation of the valon

model, allowing for momentum degradation of each of the valons independently and for changes in their flavors. The effect on the nucleon momentum distributions can be calculated and the effective degradation length deduced.

In Sec. II we determine the valon and parton distribution functions from the published distribution functions at low Q^2. The valon model for pA collisions is then discussed in Sec. III, in which momentum degradation is formulated. In Sec. IV we consider in detail the projectile fragmentation process and the subsequent process of quark recombination so that the inclusive distribution of nucleons can be calculated. The net proton and neutron distributions are then calculated and compared to the experimental data in Sec. V. Predictions for pion production in the proton fragmentation region are made in Sec. VI. The conclusion is given in Sec. VII.

II. VALON AND PARTON DISTRIBUTION FUNCTIONS

The distribution functions of valons and partons have been considered in Refs. [11, 12]. They were, however, determined by fitting the muon and neutrino scattering data of the late 70s. We now have modern parton distributions from various groups at various values of Q^2. It is therefore appropriate for us to revisit the problem and determine the valon distribution functions in light of the new parton distribution functions.

In the valon model a proton is considered to consist of three valons (UUD), which have the same flavors as the valence quarks (uud) that they individually contain. Thus a valon may be regarded as a parton cluster whose structure can be probed at high Q^2, but the structure of a nucleon itself in a low-p_T scattering problem is described in terms of the valons. As in the parton model we work in a high-momentum frame so that it is sensible to use the momentum fractions of the constituents. Reserving x for the momentum fraction of a quark, we use y to denote the momentum fraction of a valon. In this paper y never denotes rapidity. Let the exclusive valon distribution function be

$$G_{UUD}(y_1, y_2, y_3) = g\,(y_1 y_2)^\alpha y_3^\beta\,\delta(y_1 + y_2 + y_3 - 1), \tag{1}$$

where y_1 and y_2 refer to the U valons and y_3 the D valon. The delta function ensures that the three valons exhaust the momentum of the proton. The exponents α and β will be determined by the parton distribution functions. The normalization factor g is determined by requiring that the probability of finding these three valons in a proton be one, i. e.

$$\int_0^1 dy_1 \int_0^{1-y_1} dy_2 \int_0^{1-y_1-y_2} dy_3\, G_{UUD}(y_1, y_2, y_3) = 1. \tag{2}$$

Thus we have

$$g = \left[B(\alpha+1, \beta+1)B(\alpha+1, \alpha+\beta+2)\right]^{-1}, \tag{3}$$

where $B(m, n)$ is the beta function. The single valon distributions are obtained by appropriate integrations

$$G_U(y) = \int dy_2 \int dy_3 G_{UUD}(y, y_2, y_3) = gB(\alpha+1, \beta+1)y^\alpha(1-y)^{\alpha+\beta+1}, \tag{4}$$

$$G_D(y) = \int dy_1 \int dy_2 G_{UUD}(y_1, y_2, y) = gB(\alpha+1, \alpha+1)y^\beta(1-y)^{2\alpha+1}. \tag{5}$$

The two-valon distributions are trivial because of the δ-function in Eq. (1).

In a deep inelastic scattering the structure of the proton is probed to reveal the parton distributions, which in the valon model are convolutions of $G_v(y)$ with the evolution functions that describe the valon structure. The latter have two varieties: $K(z, Q^2)$ for the favored partons and $L(z, Q^2)$ for the unfavored partons. That is, u is favored in U and d is favored in D, but they are unfavored in D and U, respectively. At high Q^2 we may ignore the influence of the spectator valons when one valon is probed (the usual impulse approximation), so we can write for the u and d quark distribution functions as

$$x\,u(x, Q^2) = \int_x^1 dy \left[2G_U(y)K(x/y, Q^2) + G_D(y)L(x/y, Q^2)\right], \tag{6}$$

$$x\,d(x, Q^2) = \int_x^1 dy \left[G_D(y)K(x/y, Q^2) + 2G_U(y)L(x/y, Q^2)\right]. \tag{7}$$

It should be emphasized that $u(x)$, $d(x)$ and $G(y)$ are noninvariant distributions defined in the phase space dx and dy, while $K(z)$ and $L(z)$ are invariant distributions defined in the phase space dz/z.

The favored distribution $K(z,Q^2)$ has two parts, valence and sea, while the unfavored distribution $L(z,Q^2)$ has only sea. The valence part is also referred to as the non-singlet component, $K_{NS}(z,Q^2)$, so we may write

$$K(z,Q^2) = K_{NS}(z,Q^2) + L(z,Q^2). \tag{8}$$

At high Q^2 both K_{NS} and L can separately be determined in perturbative QCD. However, since low-Q^2 parton distributions are now available by extrapolation, and especially since we shall apply the valon model to low-p_T processes (and therefore at low Q^2), we use phenomenological forms for K_{NS} and L at low Q^2 with parameters to be determined by the low-Q^2 parton distributions. We adopt the forms

$$K_{NS}(z) = z^a(1-z)^b/B(a,b+1), \tag{9}$$

$$L(z) = \ell_o(1-z)^5, \tag{10}$$

where Eq. (9) satisfies the requirement that there is only one valence quark in a valon, i. e.

$$\int_0^1 \frac{dz}{z} K_{NS}(z) = 1. \tag{11}$$

Eq. (10) has the usual sea-quark distribution, also used previously [14].

The parton distributions that we use to fit are the ones determined by the CTEQ collaboration [16]. In particular, they have the distributions at low Q^2, labeled CTEQ4LQ, posted on the web [17]. We choose the one at $Q^2 = 1\,GeV^2$ evolved from $Q_0^2 = 0.49\,GeV^2$. We fit the $u(x,Q^2)$ and $d(x,Q^2)$ distribution functions using Eqs. (4)-(10) by varying α, β, a, b and ℓ_0. The results are shown in Fig. 1, where the CTEQ functions are in solid lines, and our fitted curves are in dotted lines. We have attempted to fit the u-quark distribution as perfectly as possible; the fit of the d-quark distribution turns out to be good only at high x. Missing the normalization of $d(x,Q^2)$ at low x is a blemish, but is acceptable since we shall use the valence quark distributions mainly in the large-x region. Besides, the reliability of an extrapolation of high-Q^2 deep inelastic scattering data to low Q^2 can always be called into question.

The parameters of the fit are

$$\alpha = 0.70, \quad \beta = 0.25, \tag{12}$$

$$a = 0.79, \quad b = -0.26, \quad \ell_0 = 0.083. \tag{13}$$

The values of α and β are not very different from the ones determined in Ref. [11] based on muon-scattering data at $Q^2 = 22.5\,GeV^2$ analyzed by Duke and Roberts [18]; there we had $\alpha = 0.65$ and $\beta = 0.35$. As can be seen from Eqs. (4) and (5), our present result means that $G_U(y) \propto (1-y)^{1.95}$ and $G_D(y) \propto (1-y)^{2.4}$ at large y, as opposed to $(1-y)^{2.0}$ and $(1-y)^{2.3}$, respectively, for the previous result. The values of a and b in Eq. (13) suggest that $K_{NS}(z,Q^2)$ is highly peaked near $z=1$, according to Eq. (9). That is as it should be, since Q^2 is only about twice the value of Q_0^2 and thus not much evolution. If there were no evolution, i. e., $Q^2 = Q_0^2$, then $K_{NS}(z,Q_0^2)$ would be $\delta(z-1)$ and $L(z) = 0$, a situation indicating no probing of the valons. What we have at $Q^2 = 1\,GeV^2$ gives only a modest degree of resolution of the valon structure, and $K_{NS}(z,Q_0^2)$ is changed from $\delta(z-1)$ to $(1-z)^{-0.26}$ in the large y region, while $L(z,Q_0^2)$ becomes non-vanishing. These are the valence and sea quark distributions that we shall use for nucleon production at low p_T in the following.

III. MOMENTUM DEGRADATION IN THE VALON MODEL

The valon model for inclusive reactions is basically a s-channel description of particle production in contradistinction from the Regge-Gribov approach [19] which is essentially based on cutting t-channel exchanges in elastic amplitudes. The two approaches are roughly complementary in that the former can best describe the fragmentation region, while the latter is more suitable for the central region.

It has been known for a long time that the pion inclusive cross section in the proton fragmentation region has a x_F dependence that is very similar to the quark distribution in the proton [20]. That similarity has been reconfirmed more recently in pA collisions by the E910 experiment [1] even at the relatively low energy of $E_{\rm lab} = 17.5 GeV$. It suggests that the proton structure is highly relevant to the spectra of particles produced in the fragmentation region.

The connection between the quark distribution and the pion inclusive distribution was first put on a calculable basis by the recombination model [13], which was subsequently improved in the framework of the valon model [12]. The idea of recombination as a basis for hadronization in hadronic collisions is eminently reasonable, since for a pion to be detected at $x_F = 0.8$, say, it is far less costly to have a quark at x_1 coalescing with an antiquark at x_2, each < 0.8, to form a pion at $x_F = x_1 + x_2$, as compared to the fragmentation process for which a quark or diquark must first have $x > 0.8$. In quark jets, fragmentation is reasonable because hadronization is initiated by a leading quark, but it is less persuasive when adapted to hadronic fragmentation unless the projectile momentum resides entirely in a quark or diquark [21, 22], contrary to Ochs' observation of the relevance of the canonical quark distributions.

The s-channel treatment of relating quark distributions to inclusive hadron distributions in pp collisions essentially regards the effect of the opposite-going initial proton as unimportant, an approximation that can only be justified in the fragmentation regions due to short-range correlation in rapidity. Thus the valon model, as it has been developed up to now, is not expected to be applicable to the central regions, where the interaction between the two incident particles is of paramount importance. For pA collisions even the factorization of the fragmentation properties is not entirely valid, since the hadron distributions are known to depend on centrality or target size. This is the problem that we shall treat in this paper in the framework of the valon model. More specifically, we shall consider the problem of momentum degradation of the valons due to the nuclear medium. Recombination occurs outside the nucleus and is therefore unaffected.

The NA49 data on p-Pb collisions are presented in terms of two mean values, $\bar{\nu}$, of the number of participating nucleons in the target: $\bar{\nu} = 6.3$ for central collisions and $\bar{\nu} = 3.1$ for non-central collisions [1]. We assume a Poissonian fluctuation from that mean with the distribution

$$P_{\bar{\nu}}(\nu) = \frac{\bar{\nu}^\nu}{\nu!}(e^{\bar{\nu}} - 1)^{-1}, \tag{14}$$

which is normalized by

$$\sum_{\nu=1}^{\infty} P_{\bar{\nu}}(\nu) = 1, \tag{15}$$

where we have excluded the $\nu = 0$ term, since it is necessary for $\nu \geq 1$ in order to have a collision. Thus ν is the number of nucleons in the nucleus that suffer inelastic collisions in any given event, ν being an integer. That is the counting on the target side, while on the projectile side we count in terms of the valons. Let the ith valon encounter ν_i collisions. In general, the total valonic collisions is bounded by

$$\nu \leq \sum_{i=1}^{3} \nu_i \leq 3\nu. \tag{16}$$

The upper bound occurs only when all three valons participate in each of the struck nucleon, while the lower limit is for only one valon per struck nucleon. In the Appendix we shall show that the data favor the lower bounds, so for simplicity we proceed in the following with the assumption

$$\nu = \nu_1 + \nu_2 + \nu_3. \tag{17}$$

It is useful to interpret this in the t-channel picture. The incident proton is represented by three constituents, each of which exchanges ν_i ladders with ν_i target nucleons so that the overall diagram is highly non-planar. Cutting the ladders gives rise to the particles produced in the s channel, mostly in the central region.

Focusing on the evolution of the valons, we first assume that the three valons interact with the target independently, since they are loosely bound to form the proton, just as the nucleons are in a deuteron. If we denote the degradation effect of the nucleus on the ith valon by $D(z_i, \nu_i)$, then we can write the evolution equation on the valon distribution as

$$y_1' y_2' y_3' G'(y_1', y_2', y_3'; \nu_1, \nu_2, \nu_3) = \int dy_1 dy_2 dy_3\, G(y_1, y_2, y_3) D(\frac{y_1'}{y_1}, \nu_1) D(\frac{y_2'}{y_2}, \nu_2) D(\frac{y_3'}{y_3}, \nu_3) \tag{18}$$

where G' is the valon distribution function after (ν_1, ν_2, ν_3) interactions with the nucleus. As in Eqs. (6) and (7), G and G' are noninvariant distributions defined in the phase space $dy_1\, dy_2\, dy_3$, etc., while $D(z_i, \nu_i)$ is an invariant distribution defined in dz_i/z_i. We postpone our discussion of what $D(z_i, \nu_i)$ is until Sec. V.

For an event with ν collisions the evolved valon distribution function $G'_\nu(y_1', y_2', y_3')$ with ν partitioned as in Eq. (17) is given by the multinomial formula

$$G'_\nu(y_1', y_2', y_3') = \frac{1}{3^\nu} \sum_{[\nu_i]} \frac{\nu!}{\nu_1! \nu_2! \nu_3!} G'(y_1', y_2', y_3'; \nu_1, \nu_2, \nu_3), \tag{19}$$

where $[\nu_i]$ implies that the summation is over ν_1, ν_2, and ν_3 subject to the constraint of Eq. (17). Note that if the nucleus had no effect on the valons, i.e.,

$$D(z_i, \nu_i) = \delta(z_i - 1) \tag{20}$$

independent of ν_i, then $G'(y'_1, y'_2, y'_3; \nu_1, \nu_2, \nu_3)$ becomes $G(y_1, y_2, y_3)$ in Eq. (18) and so does $G'_\nu(y'_1, y'_2, y'_3)$ in Eq. (19), as it should. To relate to the experimental $\bar{\nu}$, we have

$$G'_{\bar{\nu}}(y'_1, y'_2, y'_3) = \sum_\nu G'_\nu(y'_1, y'_2, y'_3) P_{\bar{\nu}}(\nu), \tag{21}$$

where $P_{\bar{\nu}}(\nu)$ is given in Eq. (14).

It is useful to introduce the notion of an effective nucleon after ν collisions by giving it a momentum fraction y' and defining the probability of finding it at y' by

$$\mathcal{G}'_\nu(y') = \int dy'_1 dy'_2 dy'_3 \, G'_\nu(y'_1, y'_2, y'_3) \, \delta(y'_1 + y'_2 + y'_3 - y') \tag{22}$$

Conservation of baryon number requires that

$$\int_0^1 dy' \mathcal{G}'_\nu(y') = 1 = \int dy'_1 dy'_2 dy'_3 \, G'_\nu(y'_1, y'_2, y'_3). \tag{23}$$

The possibility that flavor can change is a secondary issue that will be discussed later; here, the issue is that the baryon should be somewhere in the interval $0 \leq y' \leq 1$. The second half of Eq. (23) puts a constraint on $D(z_i, \nu_i)$, since we can obtain from Eqs. (18) and (2)

$$\int \frac{dz}{z} D(z, \nu_i) = 1. \tag{24}$$

The likelihood that the three evolved valons will in reality reconstitute a nucleon is extremely low, but the fictitious nucleon that they form carries a baryon number that is conserved, and a momentum that is not conserved. Indeed, we expect the average y' to decrease with ν, i. e.,

$$\bar{y}'_\nu = \int_0^1 dy' y' \mathcal{G}'_\nu(y') < 1. \tag{25}$$

That is commonly referred to as stopping. In Sec. V we shall infer from the data what the stopping power is.

Even without stopping, such as in pp collisions, it does not mean that the real proton produced cannot have $x_F < 1$. It is known that in pp collisions the proton inclusive cross section $d\sigma/dx_F$ is nearly flat in x_F. Stopping goes on top of that distribution, making it roughly exponential decrease in x_F. How to proceed from the valon distribution G' to the detected proton distribution H_p is the subject of the next section.

The convolution equation (18) can be simplified when expressed in terms of the moments on account of the convolution theorem. Thus let us define

$$\tilde{D}(n_i, \nu_i) = \int_0^1 \frac{dz_i}{z_i} z_i^{n_i - 1} D(z_i, \nu_i), \tag{26}$$

$$\tilde{G}(n_1, n_2, n_3) = \int_0^1 dy_1 \int_0^{1-y_1} dy_2 \int_0^{1-y_1-y_2} dy_3 \left[\prod_{i=1}^3 y_i^{n_i - 1} \right] G(y_1, y_2, y_3) \tag{27}$$

and similarly for $\tilde{G}'(n_1, n_2, n_3; \nu_1, \nu_2, \nu_3)$ and $\tilde{G}'_\nu(n_1, n_2, n_3)$. It then follows from Eqs. (18) and (19) that

$$\tilde{G}'_\nu(n_1, n_2, n_3) = \frac{1}{3^\nu} \sum_{[\nu_i]} \frac{\nu!}{\nu_1!, \nu_2!, \nu_3!} \tilde{G}(n_1, n_2, n_3) \prod_{i=1}^3 \tilde{D}(n_i, \nu_i). \tag{28}$$

Now, $D(n_i, \nu_i)$ itself can be described by a convolution equation [14]. If instead of the discrete ν_i we use a continuous variable L that denotes the length of the nuclear medium a valon traverses, we can express the change on $D(z, L)$ for an incremental distance dL in the form [23]

$$\frac{d}{dL} D(z, L) = \int_z^1 \frac{dz'}{z'} D(z', L) Q(z/z') \tag{29}$$

with some reasonable kernel $Q(z/z')$. In terms of the moments with

$$\tilde{Q}(n) = \int_0^1 d\zeta\, \zeta^{n-2} Q(\zeta), \tag{30}$$

Eq. (29) becomes

$$\frac{d}{dL}\tilde{D}(n,L) = \tilde{D}(n,L)\tilde{Q}(n), \tag{31}$$

whose solution is

$$\tilde{D}(n,L) = \exp\left[\tilde{Q}(n)L\right]. \tag{32}$$

The constraint (24) implies

$$\tilde{D}(1,L) = 1, \quad \text{and} \quad \tilde{Q}(1) = 0. \tag{33}$$

Since ν_i is proportional to L, let us now revert $\tilde{D}(n,L)$ to $\tilde{D}(n_i,\nu_i)$ and write Eq. (32) as

$$\tilde{D}(n_i,\nu_i) = d(n_i)^{\nu_i}, \tag{34}$$

where $d(n_i)$ is trivially related to $e^{\tilde{Q}(n_i)}$ with a power exponent whose detail need not be specified here. From Eq. (33) follows

$$d(1) = 1. \tag{35}$$

We now can use Eq. (34) in (28) and obtain

$$\tilde{G}'_\nu(n_1,n_2,n_3) = \tilde{G}(n_1,n_2,n_3)\left[\frac{1}{3}\sum_{i=1}^{3} d(n_i)\right]^\nu. \tag{36}$$

What we have derived here is that the dependence on ν is in the exponent, implying that the effects of the successive collisions with the nucleons in the target nucleus are multiplicative, as is reasonable. We can now go back to Eq. (25) and calculate the average $\bar{y}'_\nu$ after ν collisions. Using Eq. (22) we get

$$\begin{aligned}\bar{y}'_\nu &= \tilde{G}'_\nu(2,1,1) + \tilde{G}'_\nu(1,2,1) + \tilde{G}'_\nu(1,1,2) \\ &= \left[\tilde{G}(2,1,1) + \tilde{G}(1,2,1) + \tilde{G}(1,1,2)\right]\{[2+d(2)]/3\}^\nu\end{aligned} \tag{37}$$

with the help of Eqs. (35) and (36). The first factor in the square brackets is just 1, since it is

$$\int dy_1 dy_2 dy_3 (y_1+y_2+y_3) G(y_1,y_2,y_3) = \left\langle \sum_i y_i \right\rangle = 1, \tag{38}$$

which is guaranteed by the δ-function in Eq. (1). Hence, we have

$$\bar{y}'_\nu = \xi^\nu, \qquad \xi = [2+d(2)]/3 < 1. \tag{39}$$

Averaging over $P_{\bar{\nu}}(\nu)$, defined in Eq. (14), yields

$$\langle y' \rangle_{\bar{\nu}} = \sum_{\nu=1}^{\infty} \bar{y}'_\nu P_{\bar{\nu}}(\nu) = (e^{\xi\bar{\nu}} - 1)/(e^{\bar{\nu}} - 1). \tag{40}$$

This is the average momentum fraction of the effective nucleon after $\bar{\nu}$ collisions but before fragmentation into final-state particles in the fragmentation region.

IV. FRAGMENTATION AND RECOMBINATION

We now consider the problem of how a projectile proton fragments and how the quarks recombine to form the detected nucleon, thereby specifying how the inclusive distribution can be calculated. To give an overview of the procedure, let us summarize the two steps above by the two invariant distributions: $F(x_1, x_2, x_3)$, the probability of finding a u quark at x_1, another u quark at x_2, and a d quark at x_3, and $R_p(x_1, x_2, x_3, x)$, the recombination function, which specifies the probability that those three quarks coalesce to form a proton at x. How these distributions are related to the valon distributions will be discussed later. But first we state that the invariant distribution function for the detection of a proton at x is

$$\frac{x}{\sigma_{in}}\frac{d\sigma^p}{dx} \equiv H_p(x) = \frac{1}{N}\int \frac{dx_1}{x_1}\frac{dx_2}{x_2}\frac{dx_3}{x_3}F(x_1, x_2, x_3)R_p(x_1, x_2, x_3, x) \tag{41}$$

where the normalization factor N will be given below. Eq. (41) is the essence of the recombination model [12]-[14]. For meson production, only the distributions for q and $\bar{q}$ need be considered and Eq. (41) can be simplified accordingly. As in all distributions considered in this paper, color and spin components are averaged over in the initial state and summed in the final state so that we are not concerned explicitly with such degrees of freedom. Flavor, however, is different, since we identify the final-state particles by their flavors; that problem will be treated presently.

Before proceeding we emphasize what has been mentioned in the preceding section already, namely: Eq. (41) is expected to be valid in the proton fragmentation region only, if $F(x_1, x_2, x_3)$ is to be determined from the projectile valon distributions with no quarks originating from the target nucleons. In this s-channel approach, the factorization of the projectile and target fragmentations, apart from the momentum-degradation effect studied in the previous section, can be justified only if the two fragmentation regions are well separated. At AGS that is not the case. Even at SPS the central region in rapidity can encompass sizable portions of the positive and negative x_F variables. The application of the valon model to the analysis of the data therefore needs some help from the experiments.

Fortunately, the NA49 collaboration has treated their data in such a way as to eliminate the contribution of the target fragmentation from the projectile fragmentation region. From their data on the net proton produced, $p + A \to (p - \bar{p}) + X$, for which we use the abbreviated notation $(p - \bar{p})_p$, they subtract the distribution for $(p - \bar{p})_\pi$, which is $\frac{1}{2}[(p - \bar{p})_{\pi^+} + (p - \bar{p})_{\pi^-}]$. By charge conjugation symmetry, $(p - \bar{p})_\pi$ should have no projectile fragmentation, only target fragmentation. Thus the difference $(p - \bar{p})_p - (p - \bar{p})_\pi$ should have no target fragmentation [24]. With those data as our goal for analysis, Eq. (41) is then particularly suitable.

The normalization factor N in Eq. (41) is determined by requiring that the proton distribution in the absence of any target, $H_p^0(x)$, satisfies the sum rules

$$\int_0^1 \frac{dx}{x}H_p^0(x) = \int_0^1 dx H_p^0(x) = 1, \tag{42}$$

which follow from the condition that the number of proton and its momentum fraction be 1. Without any collision the quarks are identified with the unresolved valons, so $F(x_1, x_2, x_3)$ becomes

$$F^0(x_1, x_2, x_3) = x_1 x_2 x_3 G_{UUD}(x_1, x_2, x_3). \tag{43}$$

The recombination function is the time-reversed form of the valon distribution, so

$$R_p(x_1, x_2, x_3, x) = \frac{x_1 x_2 x_3}{x^3} G_{UUD}\left(\frac{x_1}{x}, \frac{x_2}{x}, \frac{x_3}{x}\right). \tag{44}$$

Putting these in Eq. (41), we obtain in view of (1)

$$H_p^0(x) = \frac{g^2}{N}\int_0^1 dx_1 \int_0^{1-x_1} dx_2 (x_1 x_2)^{2\alpha+1}(1 - x_1 - x_2)^{2\beta+1} x^{-(2\alpha+\beta+2)}\delta(x - 1). \tag{45}$$

Because of the presence of $\delta(x - 1)$, the two integrals in Eq. (42) are identical, and we get

$$N = g^2 B(2\alpha + 2, 2\alpha + 2\beta + 4)B(2\alpha + 2, 2\beta + 2). \tag{46}$$

The factor g^2, although known from Eq. (3), will cancel the similar factor that will emerge from the integral in the numerator of Eq. (41), just as they appear explicitly in Eq. (45).

The identification of the recombination function with the invariant form of the valon distribution in Eq. (44) is the principle characteristic of the valon model. On the one hand, it recognizes the role of the wave function of the proton

both in a projectile and in a produced proton. On the other hand, the momentum fractions x_i of the outgoing valons can add up to a proton at x, so there is no need for any constituent in the process to have a momentum fraction greater than x, as would be necessary in a quark fragmentation model. One may then question how in a collision process can the quarks at x_1, x_2, and x_3 in Eq. (41) become the valons of the outgoing proton. The answer is that hadronization occurs outside the target, and that the quarks moving downstream dress up themselves and become the valons of the produced proton without any change in the net momentum of each quark/valon, which is all that matters in the specification of $R_p(x_1, x_2, x_3, x)$.

We now consider the quark distribution $F(x_1, x_2, x_3)$ in Eq. (41) in pA collision before recombination. In the preceding section we have formulated the procedure to calculate the effect of the nuclear medium on the momenta of the valons as they traverse the target. Momentum degradation is, however, only one of the effects of valon-nucleon interaction. If such an interaction is represented by a Regge exchange, we should also consider the possibility of flavor changes of the valons due to non-vacuum exchanges at non-asymptotic energies. In the spirit of the s-channel approach that we have taken, in which the probabilities of occurrences at various stages are assembled multiplicatively, we assume that the flavor changes at each of the ν_i collisions are incoherent so that the net probability of a flavor change after ν_i interactions is also multiplicative. Let q be the probability of a flavor change from U to D, or from D to U, at one of the ν_i interactions. Furthermore, let q_{ν_i} be the probability of flavor change after ν_i interactions. Then q_{ν_i} satisfies the recursion relation

$$q_{\nu_i+1} = q_{\nu_i}(1-q) + (1-q_{\nu_i})q, \tag{47}$$

where the first term on the RHS denotes no change in the last step from ν_i to ν_{i+1}, while the second term denotes a change in the last step. The solution of Eq. (47) is

$$q_{\nu_i} = \frac{1}{2}[1-(1-2q)^{\nu_i}]. \tag{48}$$

We may now write what a U and a D valon become after ν_i interactions in obvious notation:

$$U \xrightarrow{\nu_i} p_{\nu_i} U + q_{\nu_i} D \tag{49}$$

$$D \xrightarrow{\nu_i} p_{\nu_i} D + q_{\nu_i} U \tag{50}$$

where $p_{\nu_i} = 1 - q_{\nu_i}$. This regeneration process depends on one parameter q. We expect q to decrease with energy $\sqrt{s}$. Here we treat it as one free parameter to fit the NA49 data at one energy $E_{\rm lab} = 158\,GeV$.

For the quark distribution in a valon we have the favored and unfavored types discussed in Sec. II, and denoted by $K(z)$ and $L(z)$, respectively. We drop the Q^2 dependence, since we now consider low-p_T hadronic processes for which there is no precise Q^2. Nevertheless, we shall use the parameterization in Eqs. (9), (10) and (13), from the $Q^2 = 1\,GeV^2$ CTEQ parton distributions. We use the following notation for the invariant distributions of quarks in valons with superscript f signifying 'favored' and u 'unfavored':

V_{ij}^f: favored quark at x_j in valon at y_i',

$W_{i,jk}^{ff}$: two favored quarks at x_j and x_k in valon at y_i'.

Other distributions involving unfavored quarks are similarly defined. Examples of V_{ij}^f, V_{ij}^u, $W_{i,jk}^{ff}$, and $W_{i,jk}^{fu}$ are depicted by diagrams in Fig. 2.

In view of Eq. (49) and Eq. (50) we can write by definition

$$V_{ij}^f = p_{\nu_i} K\left(\frac{x_j}{y_i'}\right) + q_{\nu_i} L\left(\frac{x_j}{y_i'}\right) \tag{51}$$

$$V_{ij}^u = p_{\nu_i} L\left(\frac{x_j}{y_i'}\right) + q_{\nu_i} K\left(\frac{x_j}{y_i'}\right) \tag{52}$$

$$W_{i,jk}^{ff} = p_{\nu_i}\left\{K\left(\frac{x_j}{y_i'}\right) L\left(\frac{x_k}{y_i'-x_j}\right)\right\}_{jk} + q_{\nu_i}\left\{L\left(\frac{x_j}{y_i'}\right) L\left(\frac{x_k}{y_i'-x_j}\right)\right\}_{jk} \tag{53}$$

$$W_{i,jk}^{uu} = p_{\nu_i}\left\{L\left(\frac{x_j}{y_i'}\right) L\left(\frac{x_k}{y_i'-x_j}\right)\right\}_{jk} + q_{\nu_i}\left\{K\left(\frac{x_j}{y_i'}\right) L\left(\frac{x_k}{y_i'-x_j}\right)\right\}_{jk} \tag{54}$$

$$W^{fu}_{i,jk} = p_{\nu_i}\left\{K\left(\frac{x_j}{y'_i}\right)L\left(\frac{x_k}{y'_i - x_j}\right)\right\}_{jk} + q_{\nu_i}\left\{L\left(\frac{x_j}{y'_i}\right)K\left(\frac{x_k}{y'_i - x_j}\right)\right\}_{jk} \tag{55}$$

where

$$\left\{f_1\left(\frac{x_j}{y'_i}\right)f_2\left(\frac{x_k}{y'_i - x_j}\right)\right\}_{jk} = \frac{1}{2}\left[f_1\left(\frac{x_j}{y'_i}\right)f_2\left(\frac{x_k}{y'_i - x_j}\right) + f_2\left(\frac{x_k}{y'_i}\right)f_1\left(\frac{x_j}{y'_i - x_k}\right)\right]. \tag{56}$$

In terms of these V and W distributions we can now write out, by inspection, all possible contributions to the uud quarks, shown in Fig. 3, for the production of a proton

$$\begin{aligned} M_p(y'_1, y'_2, y'_3; x_1, x_2, x_3) \;=\; & V^f_{11}V^f_{22}V^f_{33} + 2\{V^f_{11}V^u_{23}V^u_{32}\}_{12} \\ & +2\{V^f_{11}W^{fu}_{2,23}\}_{12} + 2V^u_{13}W^{ff}_{2,12} + 2\{V^f_{11}W^{fu}_{3,32}\}_{12} \\ & +2V^u_{13}W^{uu}_{3,12} + 2\{V^u_{31}W^{fu}_{1,23}\}_{12} + 2V^f_{33}W^{ff}_{1,12}, \end{aligned} \tag{57}$$

where $\{\,\}_{12}$ denotes symmetrization of x_1 and x_2. We have ignored the contributions corresponding to all three quarks coming from the same valon. The quark distribution from the proton source for proton production is then

$$F_p(x_1, x_2, x_3) = \int dy'_1 dy'_2 dy'_3\, G'_{\bar\nu}(y'_1, y'_2, y'_3) M_p(y'_1, y'_2, y'_3; x_1, x_2, x_3) \tag{58}$$

where $G'_{\bar\nu}(y'_1, y'_2, y'_3)$ is given in Eq. (21). For $\bar p$ production we need only change all K functions in Eqs. (51) - (55) to L functions, since all anti-quarks are in the sea. Denoting the corresponding quantities in Eqs. (57) and (58) by $M_{\bar p}$ and $F_{\bar p}$, we have finally for net proton production

$$F_{p-\bar p} = G'_{\bar\nu} \otimes (M_p - M_{\bar p}), \tag{59}$$

where the convolution is defined by the integral in Eq. (58). It should be recognized that $G'_{\bar\nu}(y'_1, y'_2, y'_3)$ involves a summation of $G'(y'_1, y'_2, y'_3)$ over ν, which in turn involves a summation $G'(y'_1, y'_2, y'_3; \nu_1, \nu_2, \nu_3)$ over ν_1, ν_2 and ν_3 that appear in the V and W distributions.

We are now ready to substitute $F(x_1, x_2, x_3)$ and $R(x_1, x_2, x_3, x)$, defined in Eq. (44), into Eq. (41) to calculate $H(x)$. Nine convolution integrals are involved: y_i, y'_i, and x_i. Obviously, we should go to the moments and reduce them to products. First, using Eqs. (1) in (44), we have

$$H(x) = \frac{g}{N}x^{-(2\alpha+\beta+2)}\int dx_1 dx_2 dx_3 F(x_1, x_2, x_3)(x_1 x_2)^{\alpha+1}x_3^{\beta+1}\delta(x_1 + x_2 + x_3 - x). \tag{60}$$

For convenience, let us leave out the known factors and define

$$H'(x) = \frac{N}{g}x^{2\alpha+\beta+4}H(x). \tag{61}$$

Then define the moments

$$\tilde H'(n) = \int_0^1 dx x^{n-2}H'(x), \tag{62}$$

$$\tilde F(n_1, n_2, n_3) = \int dx_1 dx_2 dx_3 \left(\prod_{i=1}^{3} x_i^{n_i - 2}\right) F(x_1, x_2, x_3). \tag{63}$$

Thus it follows

$$\tilde H'(n) = \sum_{[n_i]} \frac{n!}{n_1! n_2! n_3!}\tilde F(n_1 + \alpha + 3, n_2 + \alpha + 3, n_3 + \beta + 3). \tag{64}$$

From Eq. (58) we expect from the convolution theorem to have

$$\tilde F(n_1, n_2, n_3) = \tilde G'_{\bar\nu}(n_1, n_2, n_3)\tilde M(n_1, n_2, n_3) \tag{65}$$

where $\tilde{G}'_{\bar{\nu}}$ is given by Eq. (28), apart from the Poissonian sum of (21). However, because of the ordering of x_j relative to y'_i in Eq. (57), the simple form of (65) is valid only for the first term of $M(y'_1, y'_2, y'_3; x_1, x_2, x_3)$. For that first term, which we denote by $\tilde{F}^{(1)}$, we have

$$\tilde{F}^{(1)}(n_1, n_2, n_3) = \tilde{G}'(n_1, n_2, n_3) \prod_{i=1}^{3} [p_{\nu_i} \tilde{K}(n_i) + q_{\nu_i} \tilde{L}(n_i)], \tag{66}$$

where the subscript $\bar{\nu}$ has been omitted. The summation over ν_i in Eq. (28) for $\tilde{G}'(n_1, n_2, n_3)$ should extend over p_{ν_i} and q_{ν_i} in Eq. (66). The moments of $K(z_i)$ and $L(z_i)$ are defined as usual for the invariant distributions as

$$\tilde{K}(n_i) = \int_0^1 dz_i z_i^{n_i - 2} K(z_i). \tag{67}$$

For all other terms in Eq. (57) there are V^u_{ij} and W functions, and the simple form of Eq. (65) must be modified, especially when only two valons contribute. For notational simplicity let us define

$$\tilde{V}^f_{ij} = p_{\nu_i} \tilde{K}(n_j) + q_{\nu_i} \tilde{L}(n_j), \tag{68}$$

$$\tilde{V}^u_{ij} = p_{\nu_i} \tilde{L}(n_j) + q_{\nu_i} \tilde{K}(n_j), \tag{69}$$

$$\tilde{W}^{ff}_{i,jk} = p_{\nu_i} \{\tilde{K}(n_j, n_k) \tilde{L}(n_k)\}_{jk} + q_{\nu_i} \{\tilde{L}(n_j, n_k) \tilde{L}(n_k)\}_{jk}, \tag{70}$$

$$\tilde{W}^{uu}_{i,jk} = p_{\nu_i} \{\tilde{L}(n_j, n_k) \tilde{L}(n_k)\}_{jk} + q_{\nu_j} \{\tilde{K}(n_j, n_k) \tilde{L}(n_k)\}_{jk}, \tag{71}$$

$$\tilde{W}^{fu}_{i,jk} = p_{\nu_i} \{\tilde{K}(n_j, n_k) \tilde{L}(n_k)\}_{jk} + q_{\nu_j} \{\tilde{L}(n_j, n_k) \tilde{K}(n_k)\}_{jk}, \tag{72}$$

where $\tilde{K}(n_j, n_k)$ is defined by

$$\tilde{K}(n_j, n_k) = \int_0^1 dz z^{n_j - 2} (1 - z)^{n_k - 1} K(z) \tag{73}$$

and similarly for $\tilde{L}(n_j, n_k)$. These moments arise whenever two quarks are from the same valon, as they do for all W distributions. Take, for example, the third term in Eq. (57); we have

$$\begin{aligned}
&\tilde{F}^{(3)}(n_1, n_2, n_3) \\
&= \int_0^1 dy'_1 \int_0^{1-y'_1} dy'_2 \, G'_{UU}(y'_1, y'_2) \int \left[\prod_{i=1}^{3} dx_i x_i^{n_i - 2} \right] 2 \left\{ p_{\nu_1} p_{\nu_2} K(\frac{x_1}{y'_1}) K(\frac{x_2}{y'_2}) L(\frac{x_3}{y'_2 - x_2}) + \cdots \right\} \\
&= \int_0^1 dy'_1 \int_0^{1-y'_1} dy'_2 G'_{UU}(y'_1, y'_2) y_1'^{n_1 - 1} y_2'^{n_2 + n_3 - 2} 2 p_{\nu_1} p_{\nu_2} \\
&\quad \cdot \int_0^1 dz_1 z_1^{n_1 - 2} K(z_1) \int_0^1 dz_2 z_2^{n_2 - 2} (1 - z_2)^{n_3 - 1} K(z_2) \int_0^1 dz_3 z_3^{n_3 - 2} L(z_3) + \cdots \\
&= 2\{\tilde{G}'_{UU}(n_1, n_2 + n_3 - 1) \tilde{V}^f_{11} \tilde{W}^{fu}_{2,23}\}_{12},
\end{aligned} \tag{74}$$

where $\{\}_{12}$ here means symmetrization of n_1 and n_2, and

$$G'_{UU}(m_1, m_2) = G'_{UUD}(m_1, m_2, m_3 = 1). \tag{75}$$

Performing the same type of operations on all terms we obtain

$$\begin{aligned}
&\tilde{F}_p(n_1, n_2, n_3) \\
&= G'_{UUD}(n_1, n_2, n_3) \tilde{V}^f_{11} \tilde{V}^f_{22} \tilde{V}^f_{33} + 2\{G'_{UUD}(n_1, n_3, n_2) \tilde{V}^f_{11} \tilde{V}^u_{32}\}_{12} \tilde{V}^u_{23} \\
&\quad + 2\{G'_{UU}(n_1, n_2 + n_3 - 1) \tilde{V}^f_{11} \tilde{W}^{fu}_{2,23}\}_{12} + 2G'_{UU}(n_3, n_1 + n_2 - 1) \tilde{V}^u_{13} \tilde{W}^{fu}_{2,12} \\
&\quad + 2\{G'_{UD}(n_1, n_2 + n_3 - 1) \tilde{V}^f_{11} \tilde{W}^{fu}_{3,32}\}_{12} + 2G'_{UD}(n_3, n_1 + n_2 - 1) \tilde{V}^u_{13} \tilde{W}^{uu}_{3,12} \\
&\quad + 2\{G'_{UD}(n_2 + n_3 - 1, n_1) \tilde{W}^{fu}_{1,23} \tilde{V}^u_{31}\}_{12} + 2\{G'_{UD}(n_1 + n_2 - 1, n_3) \tilde{W}^{ff}_{1,12} \tilde{V}^f_{33}\}_{12}.
\end{aligned} \tag{76}$$

Substituting this in Eq. (64), we have the final form for the moments $\tilde{H}'_p(n)$. For $\bar{p}$ production we need only change all $\tilde{K}$ in Eqs. (68) - (72) to $\tilde{L}$.

For the production of neutron the recombination function is

$$R_n(x_1,x_2,x_3,x) = \frac{x_1x_2x_3}{x^3} G_{DDU}\left(\frac{x_1}{x},\frac{x_2}{x},\frac{x_3}{x}\right), \tag{77}$$

where we use y_1 and y_2 to refer to D and y_3 to U, so the dependence of $G_{DDU}(y_1,y_2,y_3)$ on y_i is the same as that of $G_{UUD}(y_1,y_2,y_3)$ given in Eq. (1). The quark distribution $F_n(x_1,x_2,x_3)$ with the corresponding identification of x_1 and x_2 with the d quark, and x_3 with the u quark, also has eight terms, as shown in Fig. 4. We can write, by inspection, the moments $\tilde{F}_n(x_1,x_2,x_3)$ similar to Eq. (76)

$$\begin{aligned}
&\tilde{F}_n(x_1,x_2,x_3) = \\
&2\{\tilde{G}'_{UUD}(n_3,n_1,n_2)\tilde{V}^f_{13}\tilde{V}^u_{21}\tilde{V}^u_{32}\}_{12} + \tilde{G}'_{UUD}(n_1,n_2,n_3)\tilde{V}^u_{11}\tilde{V}^u_{22}\tilde{V}^u_{33} \\
&+2\tilde{G}'_{UU}(n_3,n_1+n_2-1)\tilde{V}^f_{13}\tilde{W}^{uu}_{2,12} + 2\{\tilde{G}'_{UU}(n_1,n_2+n_3-1)\tilde{V}^u_{11}\tilde{W}^{fu}_{2,32}\}_{12} \\
&+2\tilde{G}'_{UD}(n_3,n_1+n_2-1)\tilde{V}^f_{13}\tilde{W}^{ff}_{3,12} + 2\{\tilde{G}'_{UD}(n_1,n_2+n_3-1)\tilde{V}^u_{11}\tilde{W}^{fu}_{3,23}\}_{12} \\
&+2\tilde{G}'_{UD}(n_1+n_2-1,n_3)\tilde{W}^{uu}_{1,12}\tilde{V}^u_{3,3} + 2\{\tilde{G}'_{UD}(n_1+n_3-1,n_2)\tilde{W}^{fu}_{1,31}\tilde{V}^f_{3,2}\}_{12}.
\end{aligned} \tag{78}$$

Substituting this in Eq. (64) gives $\tilde{H}'_n(n)$. For $\bar{n}$ production simply replace all $\tilde{K}$ in $\tilde{H}'_n(n)$ by $\tilde{L}$.

Finally for net nucleon production we have

$$\tilde{H}'_{p-\bar{p}}(n) = \tilde{H}'_p(n) - \tilde{H}'_{\bar{p}}(n), \tag{79}$$

$$\tilde{H}'_{n-\bar{n}}(n) = \tilde{H}'_n(n) - \tilde{H}'_{\bar{n}}(n). \tag{80}$$

We shall use these in the next section to determine the x dependences to be compared with the data.

V. NET PROTON AND NEUTRON DISTRIBUTIONS

Before we can compute the distributions $H(x)$, we need to specify quantitatively the degradation function $D(z_i,v_i)$ introduced in Eq. (18) and discussed between Eq. (29) and (35). We proposed an evolution equation for $D(z,L)$ in Eq. (29) but left the kernel $Q(z/z')$ unspecified. Now, to proceed we must specify $Q(\zeta)$, which is uncalculable because it represents the non-perturbative effect of the nuclear medium on a valon as it propagates an incremental distance. We shall use an one-parameter description of the effect, so we shall be approximate by assuming that the effect is like a one-gluon exchange [14], i. e.,

$$Q(\zeta) = \frac{\kappa\zeta}{(1-\zeta)_+}, \tag{81}$$

where the singularity at $\zeta = 1$ is regularized by the subtraction

$$\frac{1}{(1-\zeta)_+} = \frac{1}{1-\zeta} - \delta(\zeta-1)\int_0^1 \frac{dx}{1-x}. \tag{82}$$

Evidently, Eq. (81) satisfies the condition

$$\int_0^1 \frac{d\zeta}{\zeta} Q(\zeta) = 0, \tag{83}$$

which is required by the constraint $\tilde{Q}(1) = 0$ stated in Eq. (33) that follows from baryon conservation. From the definition of the moments given in Eq. (30) we find, using Eq. (81),

$$\tilde{Q}(n) = -\kappa\sum_{j=1}^{n-1} = -\kappa[\psi(n)+\gamma_E], \tag{84}$$

where $\psi(n)$ is the digamma function and γ_E is the Euler's constant, 0.5722. Substituting $\tilde{Q}(n)$ into Eq. (32), and changing L to ν_i that involves a constant factor, thereby effecting a change from one unknown parameter κ to another, k, we obtain the form for $\tilde{D}(n_i, \nu_i)$ in Eq. (34) with

$$d(n_i) = \exp\{-k[\psi(n_i) + \gamma_E]\}. \tag{85}$$

This is a one-parameter description of the effect of momentum degradation. We shall vary k to fit the data. Eq. (85) is a rigorous consequence of a simple form for $Q(\zeta)$ given in Eq. (81), whose reliability is unknown. The validity of $d(n_i)$ as expressed in Eq. (85) can only be inferred *a posteriori* from the fit of the data. The exponential dependence on the degradation strength k follows only from the linear dependence of $Q(\zeta)$ on κ, and is sensible.

We have only two free parameters, k and q, to vary to fit the NA49 data on p-$\bar{p}$ and n-$\bar{n}$ [1]. Recall that q is introduced in Eq. (47) in connection with flavor changes. We repeat that the data do not include target fragmentation because $(p-\bar{p})_\pi$ and $(n-\bar{n})_\pi$ have been subtracted out. Thus the data represent only proton fragmentation and are ideal for our analysis by $H_{p-\bar{p}}(x)$ and $H_{n-\bar{n}}(x)$.

Since the data are in the x variable, we must make the inverse transformation from our moments to $H(x)$. Instead of making the inverse Mellin transform, let us exploit the orthogonality of the Legendre polynomials and shift the variable to the interval $0 \le x \le 1$. Thus, define

$$g_\ell(x) = P_\ell(2x-1) \tag{86}$$

so that

$$\int_0^1 dx g_\ell(x) g_m(x) = \frac{1}{2\ell+1}\delta_{\ell m}. \tag{87}$$

If we expand the distribution $H'(x)$ in terms of $g_\ell(x)$

$$H'(x) = \sum_{\ell=0}^{\infty}(2\ell+1)h_\ell g_\ell(x), \tag{88}$$

then the inverse is

$$h_\ell = \int_0^1 dx H'(x) g_\ell(x). \tag{89}$$

These h_ℓ can be expressed in terms of the moments $H'(n)$ if we express $g_\ell(x)$ as a power series in x

$$g_\ell(x) = \sum_{i=0}^{\ell} a_\ell^i x^i, \tag{90}$$

where a_ℓ^i are known from the properties of $P_\ell(z)$. Thus from Eq. (89) we have

$$h_\ell = \sum_{i=0}^{\ell} a_\ell^i \tilde{H}'(i+2), \tag{91}$$

where $\tilde{H}'(n)$ is defined in Eq. (62). It is now clear that our theoretical results in $\tilde{H}'(n)$ can be transformed to $\tilde{H}'(x)$ through Eqs. (88) and (91) once we have the coefficients a_ℓ^i. Furthermore, if $\tilde{H}'(n)$ becomes unimportant for $n > N$, then the sum in Eq. (88) can terminate at N.

To determine a_ℓ^i, we make use of the recursion formula

$$(\ell+1)P_{\ell+1}(z) = (2\ell+1)zP_\ell(z) - \ell P_{\ell-1}(z) \tag{92}$$

to infer through Eqs. (86) and (90)

$$a_\ell^0 = -\frac{1}{\ell}[(2\ell-1)a_{\ell-1}^0 + (\ell-1)a_{\ell-2}^0], \tag{93}$$

$$a_\ell^i = -\frac{1}{\ell}[(2\ell-1)(a_{\ell-1}^i - 2a_{\ell-1}^{i-1}) + (\ell-1)a_{\ell-2}^i], \tag{94}$$

where $\ell \geq 2$, and $1 \leq i \leq \ell$. For $i = 0$ and/or $\ell < 2$, we have

$$a_0^0 = 1, \qquad a_1^0 = -1, \qquad a_1^1 = 2. \tag{95}$$

With these we can generate all a_ℓ^i, so h_ℓ can be directly computed.

Summarizing our procedure, we calculate $\tilde{H}'_{p-\bar{p}}(n)$ and $\tilde{H}'_{n-\bar{n}}(n)$, substitute them in Eq. (91) and then (88), and then use Eq. (61) to determine $H_{p-\bar{p}}(x)$ and $H_{n-\bar{n}}(x)$. We vary k and q to fit the data of NA49 shown in Fig. 5. The inclusive distribution dN/dx_F corresponds to our $H(x)/x$. The solid lines are our results for $p - \bar{p}$ and the dashed line $n - \bar{n}$ for both $\bar{\nu} = 3.1$ and 6.3. The values of the parameters adjusted are

$$k = 0.62, \qquad\qquad q = 0.37. \tag{96}$$

The most striking aspect of our result is that the normalization of the calculated distributions turns out to be correct, even though we have no free parameter to adjust that. The degradation strength k affects the shape of the distributions and the flavor-flip probability q affects the difference between $p - \bar{p}$ and $n - \bar{n}$. The agreement between theory and experiment is fairly good, considering that we have only two free parameters and that the experimental errors (a typical size of which is shown in the figure) are large, especially at large x. The shapes of the distributions for $p - \bar{p}$ are reasonably well reproduced and so is the dependence on $\bar{\nu}$. For $n - \bar{n}$ the calculated curves are somewhat steeper than the data. However, there exist some data points for $n - \bar{n}$ above $x = 0.8$ that are significantly lower, though with much larger errors. Taken as a whole the agreement is satisfactory. Thus we conclude that the physical process of proton fragmentation and the nucleon momentum spectra are well understood in the framework of the valon model.

We can determine from the value of k what the momentum degradation length is. First, we get from Eq. (85)

$$d(2) = e^{-k} = 0.54 \tag{97}$$

for $k = 0.62$, since $\psi(2) + \gamma_E = 1$. By definition Eq. (39) we obtain $\xi = 0.85$. Inserting this in Eq. (40) we obtain a dependence of $\langle y' \rangle_{\bar{\nu}}$ on $\bar{\nu}$ that can be well approximated by

$$\langle y' \rangle_{\bar{\nu}} \propto e^{-(1-\xi)\bar{\nu}}, \tag{98}$$

for $\bar{\nu} \geq 2$. This gives the fractional momentum loss per collision

$$\frac{1}{\langle y' \rangle_{\bar{\nu}}} \frac{d}{d\bar{\nu}} \langle y' \rangle_{\bar{\nu}} = -(1 - \xi) = -0.15. \tag{99}$$

If we related $\bar{\nu}$ to average nuclear path length L by $\bar{\nu} = \sigma_{pp} t_A$ and $t_A = A\rho L$, where $\rho = \frac{4\pi}{3} R_A^3$, then for $\sigma_{pp} = 30$mb we have $\bar{\nu} \simeq 0.4L$ with L in fm. Thus, if we define the degradation length Λ by

$$\langle y' \rangle = e^{-L/\Lambda}, \tag{100}$$

then

$$\Lambda = [0.4(1 - \xi)]^{-1} \simeq 17\,\text{fm}. \tag{101}$$

This gives an estimate of how far a proton must travel in a nuclear medium in order to lose its momentum by a factor of e^{-1}.

The value of $q = 0.37$ for flavor-flip probability may at first sight appear to be surprisingly large. However, if it is regarded as an effective way of accounting for resonance production, it becomes quite acceptable. To see that, we first state that resonance production, which we have not taken into account explicitly, can easily produce neutron from $|uud\rangle$ through $\Delta^+ \to n + \pi^+$. The process can be depicted by a dual diagram, as shown in Fig. 6(a). Such a leakage of + charge through the emission of π^+ is equivalent to a flavor flip, which changes UUD to DUD, symbolized by a square box in Fig. 6(b), and the favored process, for example, of having valence quarks changes from uud to dud. Since a consideration of resonance production would involve masses, threshold, polarization, decay distribution, and other complications, our method of using flavor changes to account for the effect presents considerable technical economy. Even though resonance production can occur only at hadronization in the end charge leakage can take place at any point where a projectile valon interacts with the target; hence, the consideration in Sec. IV leading up to Eq. (50) is an effective way to take such subprocesses into account.

VI. PION PRODUCTION

Having successfully computed the nucleon distributions, resulting in the determination of the only two free parameters in the model, we are now able to predict the pion distributions without any further ambiguities. The NA49 data presented in Ref. [1] do not include the pion spectra. The E910 data [1] do have the pion distributions in the proton fragmentation region; however, being at $E_{\rm lab} = 12\,GeV$ the energy is too low to avoid substantial spill-over of quarks and produced hadrons from target fragmentation into the $x > 0$ region. Without the target fragmentation being subtracted, as is done for $p - \bar{p}$ in the NA49 data, the E910 data cannot be compared to the predictions from our model. We present our result below for a future comparison.

The invariant distribution for pion production is

$$\frac{x}{\sigma_{\rm in}}\frac{d\sigma^\pi}{dx} \equiv H_\pi(x) = \int \frac{dx_1}{x_1}\frac{dx_2}{x_2} F_\pi(x_1, x_2) R_\pi(x_1, x_2, x) \tag{102}$$

where $F_\pi(x_1, x_2)$ is the invariant distribution for finding a quark at x_1 and an antiquark at x_2, and R_π is the corresponding recombination function to form a pion. An important aspect about pion production concerns the role of gluons, a subject that will be discussed below in connection with $L(z)$. For now, we consider the appropriate forms for F_π and R_π.

We begin with the valon distribution $G'_{\bar{\nu}}(y'_1, y'_2, y'_3)$, as given by Eq. (21). As before, we shall omit the subscript $\bar{\nu}$, and replace it by the valon labels so that for the two-valon distributions we have

$$G'_{UU}(y'_1, y'_2) = \int_0^1 dy'_3 G'_{UUD}(y'_1, y'_2, y'_3), \tag{103}$$

and similarly for $G'_{UD}(y'_1, y'_3)$ by integrating out y'_2. The single-valon distributions are involved in the 5 subprocesses that contribute to $F_\pi(x_1, x_2)$ shown in Fig. 7 for the production of π^+. Of course, because of the flavor changes, the valon labels are only indicative of the unchanged components. More precisely, we can express F_π in the moment form, as in Eq. (76), for π^+

$$\begin{aligned}\tilde{F}_{\pi^+}(n_1, n_2) \;=\; & [\tilde{G}'_{UU}(n_1, n_2) + 2\tilde{G}'_{UD}(n_1, n_2)]\{\tilde{V}^f_{11}\tilde{V}^u_{22}\}_{12} \\ & + 2\tilde{G}'_{UD}(n_2, n_1)\{\tilde{V}^u_{12}\tilde{V}^u_{21}\}_{12} + 2\tilde{G}'_U(n_1 + n_2 - 1)\tilde{W}^{fu}_{1,12} \\ & + 2\tilde{G}'_D(n_1 + n_2 - 1)\tilde{W}^{uu}_{3,12},\end{aligned} \tag{104}$$

and for π^-

$$\begin{aligned}\tilde{F}_{\pi^-}(n_1, n_2) \;=\; & \tilde{G}'_{UU}(n_1, n_2)\tilde{V}^f_{11}\tilde{V}^u_{22} \\ & + 2\tilde{G}'_{UD}(n_2, n_1)\{\tilde{V}^f_{21}\tilde{V}^u_{12}\}_{12} + 2\tilde{G}'_{UD}(n_1, n_2)\{\tilde{V}^f_{11}\tilde{V}^u_{22}\}_{12} \\ & + 2\tilde{G}'_U(n_1 + n_2 - 1)\tilde{W}^{uu}_{1,12} + 2\tilde{G}'_D(n_1 + n_2 - 1)\tilde{W}^{fu}_{3,12}.\end{aligned} \tag{105}$$

For the recombination function we have

$$R_\pi(x_1, x_2, x) = \frac{x_1 x_2}{x^2} G^\pi_{U\bar{D}}\left(\frac{x_1}{x}, \frac{x_2}{x}\right), \tag{106}$$

where $G^\pi_{U\bar{D}}(y_1, y_2)$ is the valon distribution in a pion. For the latter we adopt the same form derived in Ref. [12]

$$G^\pi_{U\bar{D}}(y_1, y_2) = \delta(y_1 + y_2 - 1), \tag{107}$$

which satisfies

$$\int_0^1 dy_1 \int_0^{1-y_1} dy_2 G^\pi_{U\bar{D}}(y_1, y_2) = \int_0^1 dy_1 \int_0^{1-y_1} dy_2 (y_1 + y_2) G^\pi_{U\bar{D}}(y_1, y_2) = 1. \tag{108}$$

Consequently, the structure function of the pion $\mathcal{F}_\pi(x)$, that is related to the single-valon distribution $G^\pi_U(y)$

$$\mathcal{F}_\pi(x) \propto \int_x^1 dy G^\pi_U(y) \tag{109}$$

behaves at large x as $(1 - x)^1$, in agreement with the counting rule $(1 - x)^{2r-1}$, where r is the number of residual quarks ($r = 1$ for pion and $r = 2$ for proton).

Using Eqs. (106) and (107) in (102) yields

$$H_\pi(x) = \frac{1}{x}\int_0^1 dx_1 \int_0^{1-x_1} dx_2 F_\pi(x_1, x_2)\delta(x_1 + x_2 - x). \tag{110}$$

By defining

$$H'_\pi(x) = x^3 H_\pi(x), \tag{111}$$

we then have for the moments [see Eq. (62)]

$$\begin{aligned}\tilde{H}'_\pi(n) &= \int_0^1 dx_1 \int_0^{1-x_1} dx_2 F_\pi(x_1, x_2)(x_1 + x_2)^n \\ &= \sum_{[n_i]} \frac{n!}{n_1! n_2!}\tilde{F}_\pi(n_1, n_2), \qquad n = n_1 + n_2,\end{aligned} \tag{112}$$

whereupon Eqs. (104) and (105) can be used for the production of π^+ and π^-, respectively. The inverse transform can be done as before, using Eqs. (88) and (91).

Having formulated the procedure to calculate the pion distribution in the projectile fragmentation region, we must confront one final issue on the role of the gluons. Although the gluons carry roughly half the momentum of a proton, no glueball has ever been seen. They therefore hadronize by converting to $q\bar{q}$ pairs, which subsequently form pions. We take them into account by enhancing the sea to saturate the momentum sum rule [25]. That is, for the purpose of pion production we revise the normalization of the quark distribution $L(z)$ such that $q\bar{q}$ in the sea carry all the momentum of the incident proton apart from the momenta of the valence quarks, leaving nothing for the gluons. The average momentum fraction carried by the valence quark in a valon is

$$\langle z\rangle_{\rm val} = \int_0^1 dz K_{NS}(z) = \frac{a}{a+b+1}, \tag{113}$$

where Eq. (9) has been used. If we denote the saturated sea distribution by

$$L_1(z) = \ell_1(1-z)^5, \tag{114}$$

where only the constant factor ℓ_1 has changed from Eq. (10), then each sea quark carries on average a momentum fraction of $\ell_1/6$. That is to be identified with $(1 - \langle z\rangle_{\rm val})/2f$, where f is the number of flavors. From Eq. (13) we have $\langle z\rangle_{\rm val} = 0.52$. Setting $f = 3$, we get

$$\ell_1 = 0.48\,. \tag{115}$$

With this value in $L_1(z)$, which is then used in Eqs. (51) - (55) in place of $L(z)$, we obtain the appropriate V and W functions that should be used for the calculation of $\tilde{F}_{\pi^\pm}$ in Eqs. (104) - (105).

Evidently, there are no parameters to adjust for the calculation of the pion distributions. The results are shown in Fig. 8 for π^+ and π^- separately at $\bar{\nu} = 3.1$ and 6.3. For ease of comparison between π^+ and π^- the same curves are replotted in Fig. 9, where the charge and $\bar{\nu}$ dependences are grouped differently. No data points are included because none correspond to proton fragmentation only and at the $\bar{\nu}$ considered, as discussed at the beginning of this section. Nevertheless, if one compares our results to the data of E910 shown in [1], there is rough agreement, both in normalization and in shape. Generally speaking, the difference between π^+ and π^- diminishes as $\bar{\nu}$ is increased, though not as rapidly as in the E910 data at $E_{\rm lab} = 12GeV$. We are confident that our predictions will agree well with the data when they become available, since the pion distributions have always demonstrated the reliability of the recombination model [12, 13].

VII. CONCLUSION

We have formulated the projectile fragmentation problem in pA collisions in the valon model. Despite the non-perturbative aspect of the problem, the formulation results in a well-defined procedure of calculating various contributions to the nucleon and meson distributions in the proton fragmentation region. The nuclear target effects, which present the only unknown in the model, are summarized by two parameters k and q. They are determined by

fitting $p - \bar{p}$ and $n - \bar{n}$ distributions for two values of $\bar{\nu}$. With those parameters fixed, the predictions for the pion distributions can be calculated without any other adjustable parameters.

The results of our calculations have shown that the NA49 data can be well described by the valon model. The normalization of the nucleon spectra turns out to be correct without any freedom for adjustment. The shapes of the distributions are also acceptably reproduced. The inferred value of k that gives a quantitative measure of momentum degradation can be translated to a degradation length Λ in the form $e^{-L/\Lambda}$ for the degraded momentum fraction with $\Lambda \simeq 17$ fm.

While a value for Λ can serve as a succinct numerical summary of the stopping effect of the nucleus, we admit that it cannot be inferred directly from the pA collision data without a detailed analysis in the framework of the valon model. This aspect of the problem is worthy of further attention in the hope that a degradation length can be extracted by an appropriate model-independent analysis of the data on nucleon inclusive cross section.

It should be noted that since the valon model does not make explicit use of Regge exchanges, it is not capable of predicting the energy dependence. It is a model that should be applied only at asymptotic energies where scaling behavior prevails. To compensate for that drawback, it makes possible the s-channels approach to the calculation of the fragment distributions.

There are obvious directions into which this work can be extended. One is to incorporate strangeness and study the distributions of hyperons and kaons. Another is to generalize from pA to AA collisions. From the properties of degradation that this work has revealed, one is better positioned to assess the extent to which nuclear matter can be compressed in AA collisions. Furthermore, with some knowledge about strangeness production in pA collisions, one can determine for AA collisions how much strangeness enhancement is normal and how much anomalous.

Although the valon model represents an approach to multiparticle production that appears to be orthogonal to most other approaches based on strings, it should be recognized that the s-channel and t-channel approaches are complementary, not contradictory. One may be able to identify diagrams in Figs. 3 and 4 that correspond to baryon junction or diquark breaking. Just as the notion of duality has benefitted the investigation of high-energy processes many years ago that found its idealization in the form of Veneziano amplitude, which has perfect s- and t-channel symmetry, so also here in nuclear processes the exploration of complementary descriptions of common as well as unusual phenomena can help to elucidate the underlying dynamics responsible for them.

Acknowledgment

We are grateful to G. Veres for a helpful communication. This work was supported, in part, by the U. S. Department of Energy under Grant No. DE-FG03-96ER40972.

[1] B. Cole, talk given at Quark Matter 2001, 15th Int. Conf. on Ultra-Relativistic Nucleus-Nucleus Collision, Stony Brook, NY January 2001.
[2] R. C. Hwa, Phys. Rev. Lett. **52**, 492 (1984).
[3] L. P. Csernai, and J. I. Kapusta, Phys. Rev. D. **29**, 2664 (1984).
[4] J. Hüfner and A. Klar, Phys. Lett. B**145**, 167 (1984).
[5] C. Y. Wong, Phys. Rev. Lett. **52**, 1393 (1984).
[6] B. Z. Kopeliovich and B. G. Zakharov, Z. Phys. C **43**, 241 (1989); A. Capella and B. Z. Kopeliovich, Phys. Lett. B**381**, 325 (1996).
[7] D. Kharzeev, Phys. Lett. B**378**, 238 (1996).
[8] S. E. Vance, M. Gyulassy and X.-N. Wang, Phys. Lett. B**443**, 45 (1998).
[9] R. C. Hwa, Nucl. Phys. B (Proc. Suppl.) **92**, 348 (2001).
[10] R. C. Hwa, Phys. Rev. D**22**, 759 (1980).
[11] R. C. Hwa, and M. S. Zahir, Phys. Rev. D**23**, 2539 (1981).
[12] R. C. Hwa, Phys. Rev. D**22**, 1593 (1980).
[13] K. P. Das and R. C. Hwa, Phys. Lett. **68B**, 459 (1977).
[14] R. C. Hwa, and M. S. Zahir, Phys. Rev. D**31**, 499 (1985).
[15] D. S. Barton *et. al.*, Phys. Rev. D**27**, 2580 (1983).
[16] CTEQ Collaboration, H. L. Lai, *et. al.*, Phys. Rev. D**51**, 4763 (1995).
[17] CTEQ4LQ, http://zebu.uoregon.edu/∼parton/partongraph.html.
[18] D. Duke and R. G. Roberts, Phys. Lett. **85B**, 289 (1979).
[19] V. N. Gribov, Sov. Phys.- JETP **30**, 709 (1970).
[20] W. Ochs, Nucl. Phys. **B118**, 397 (1977).
[21] B. Andersson, G. Gustafson, and C. Peterson, Phys. L. **60B**, 221 (1977).

[22] A. Capella, U. Sukhatme, C. I. Tan and J. Tran Thanh Van, Phys. L. **81B**, 68 (1979).
[23] R. C. Hwa, J. Pišút, and N. Pišútová, Phys. Rev. Lett. **85**, 4008 (2000).
[24] We thank G. Veres for private communication on this point.
[25] D. W. Duke and F. E. Taylor, Phys. Rev. D**17**, 1788 (1978).

APPENDIX A: APPENDIX

In Sec. III we have considered the problem of describing ν collisions with the target nucleons in terms of the number of collisions that each valon experiences. With the ith valon encountering ν_i collisions, the sum $\sum_i \nu_i$ satisfies the bounds given in Eq. (16). In this Appendix we investigate the phenomenological preference for that sum within that range.

Let us define the integer μ by

$$\mu = \nu_1 + \nu_2 + \nu_3 \tag{A1}$$

so that μ is bounded by

$$\nu \leq \mu \leq 3\nu. \tag{A2}$$

Since at least one valon must interact with the nucleus, let that valon be $i = 1$. Let p be the probability that either one of the other two valons also interacts. Furthermore, let $B_\nu(\mu)$ denote the probability that out of ν independent collisions the target nucleons encounter, μ valonic collisions occur. For $\nu = 1$, we have $B_1(1) = (1-p)^2, B_1(2) = 2p(1-p)$ and $B_1(3) = p^2$, which count the probabilities that valons $i = 2$ and 3 interact in addition to the $i = 1$ valon. Generalizing that to ν collisions, we have

$$B_\nu(\mu) = \binom{2\nu}{j} p^j (1-p)^{2\nu-j}, \qquad j = \mu - \nu, \tag{A3}$$

which is a binomial distribution of having $\mu - \nu$ valonic collisions by the $i = 2$ and 3 valons out of a maximum of 2ν possible such collisions. We can define a generating function from $B_\nu(\mu)$:

$$S_\nu(z) = \sum_{\mu=\nu}^{3\nu} z^\mu B_\nu(\mu) = z^\nu \sum_{j=0}^{2\nu} z^j \binom{2\nu}{j} p^j (1-p)^{2\nu-j} = z^\nu (1-p+pz)^{2\nu} = [S_1(z)]^\nu. \tag{A4}$$

The above consideration can now be applied to Eq. (36) where $\tilde{G}'_\nu(n_1, n_2, n_3)$ is related to $\tilde{G}(n_1, n_2, n_3)$ under the assumption of Eq. (17), i. e., $\nu = \nu_1 + \nu_2 + \nu_3$. That assumption is now liberated by Eq. (A1) and (A2). The factor $[\sum_{i=1}^3 d(n_i)/3]^\nu$ in Eq. (36) should thus be replaced by $[S_1(z)]^\nu$, which allows μ to vary between ν and 3ν. In the limit $p = 0, S_1(z)$ becomes z and we recover the earlier result, if we identify

$$z = \frac{1}{3} \sum_{i=1}^{3} d(n_i). \tag{A5}$$

Using (A4) in Eq. (36), we finally have, with the help of Eq. (21)

$$\begin{aligned} \tilde{G}'_{\bar{\nu}}(n_1, n_2, n_3) \;&=\; \sum_{\nu=1}^{\infty} \tilde{G}(n_1, n_2, n_3) B_\nu(\nu_1 + \nu_2 + \nu_3) P_{\bar{\nu}}(\nu) \\ &\quad \cdot \left(\frac{1}{3}\right)^{\nu_1+\nu_2+\nu_3} \frac{(\nu_1 + \nu_2 + \nu_3)!}{\nu_1! \nu_2! \nu_3!} \prod_{i=1}^{3} d(n_i)^\nu. \end{aligned} \tag{A6}$$

The summation over ν_i is included in the sum in Eq. (28) but without the restriction of (17).

We have used the $\tilde{G}'_{\bar{\nu}}$ given in (A6) to calculate $H'(x)$ for $p - \bar{p}$ and $n - \bar{n}$, as in Secs. IV and V. The only difference from before is that we now have one additional parameter p in (A2) to adjust, which controls the number of valonic collisions above $\mu = \nu$. Our best fit of the data, as in Fig. 5, yields $p = 0.05$ with the values of k and q being essentially the same as in Eq. (96). Since p is so small, any contribution from μ different from ν can be neglected. Thus it is the data that instruct us on the suitable range of values of ν_i, namely: $\nu_1 + \nu_2 + \nu_3$ is dominantly at its lower bound ν.

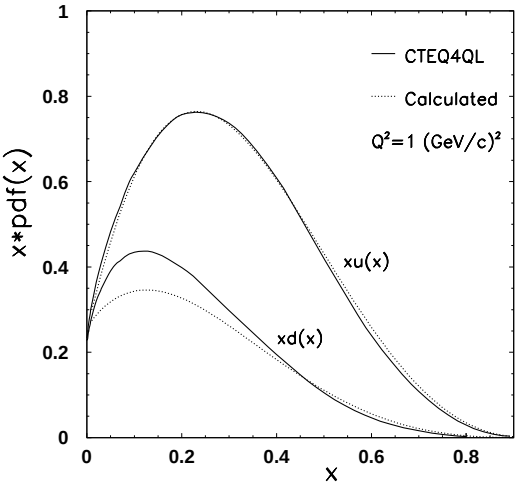


FIG. 1: Parton distribution functions at $Q^2 = 1\,(\mathrm{GeV/c})^2$. The solid lines are from CTEQ4QL [16], and the dotted lines are from our calculation.

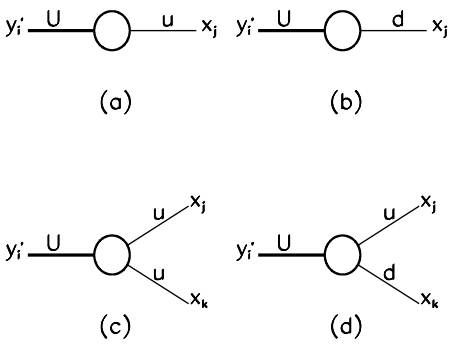


FIG. 2: (a) V_{ij}^{f}, favored quark in a valon, (b) V_{ij}^{u}, unfavored quark in a valon, (c) $W_{i,jk}^{ff}$, two favored quarks in a valon, (d) $W_{i,jk}^{fu}$, a favored and an unfavored quark in a valon.

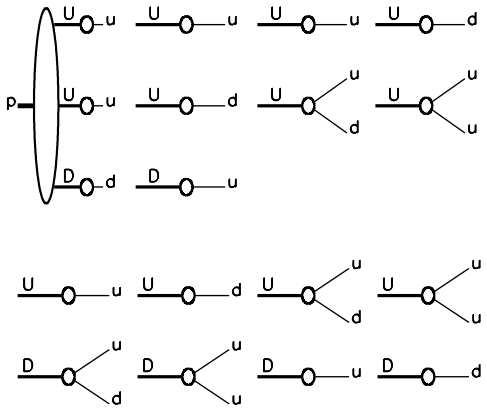


FIG. 3: Eight types of contributions to the quark state *uud* in a proton.

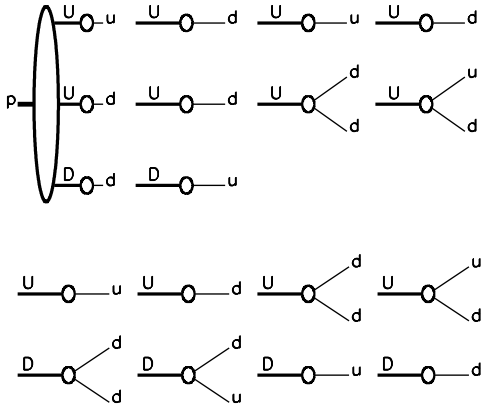


FIG. 4: Eight types of contributions to the quark state *udd* in a proton.

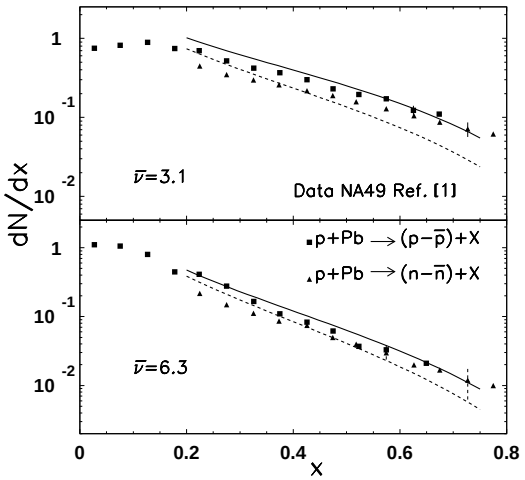


FIG. 5: Inclusive distributions for the production of $p - \bar{p}$ (solid) and $n - \bar{n}$ (dashed) in p-Pb collisions. The data are from NA49, reported in [1].

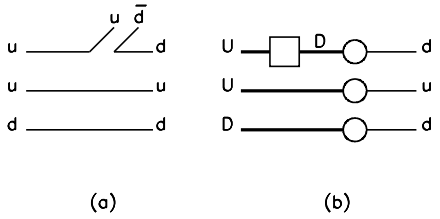


FIG. 6: (a) A dual diagram that represents the process $\Delta^+ \to n + \pi^+$. (b) The square box symbolizes a flavor change from U valon to D valon before the quark momenta are determined in the valon model.

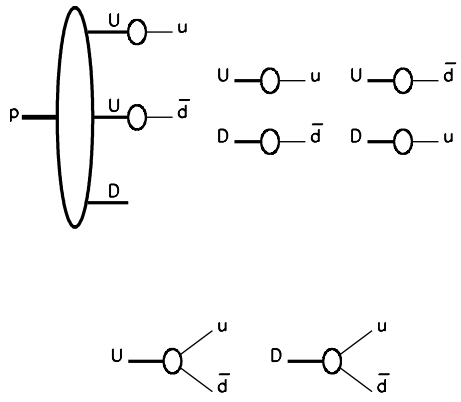


FIG. 7: Five types of contributions to the quark state $u\bar{d}$ in a proton.

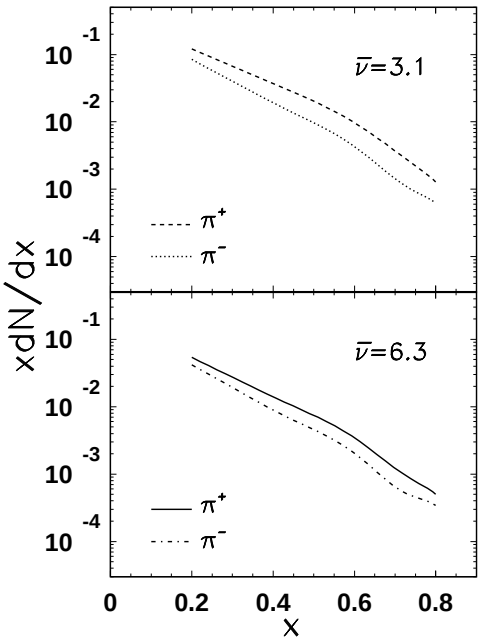


FIG. 8: Inclusive pion distributions of π^+ and π^- at $\bar{\nu} = 3.1$ and 6.3.

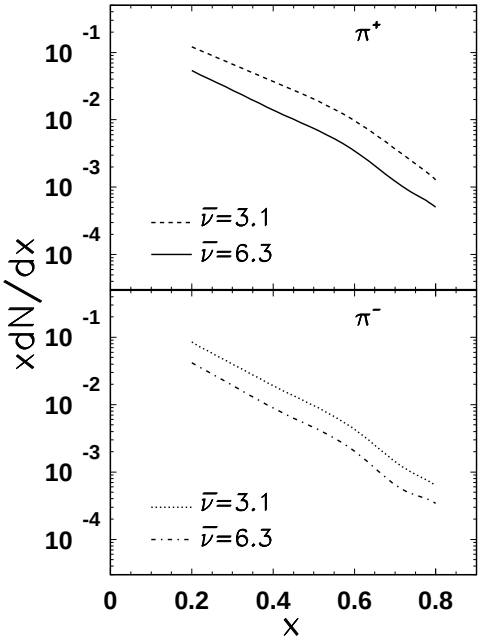


FIG. 9: Same as in Fig. 8 but grouped differently.